

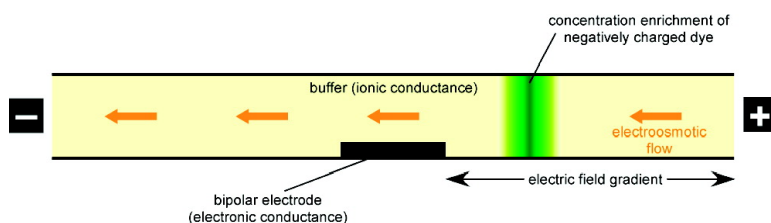
Communication

Electrokinetics in Microfluidic Channels Containing a Floating Electrode

Rahul Dhopeswarkar, Dzmitry Hlushkou, Mark Nguyen, Ulrich Tallarek, and Richard M. Crooks

J. Am. Chem. Soc., **2008**, 130 (32), 10480-10481 • DOI: 10.1021/ja8036405 • Publication Date (Web): 22 July 2008

Downloaded from <http://pubs.acs.org> on February 8, 2009



More About This Article

Additional resources and features associated with this article are available within the HTML version:

- Supporting Information
- Links to the 1 articles that cite this article, as of the time of this article download
- Access to high resolution figures
- Links to articles and content related to this article
- Copyright permission to reproduce figures and/or text from this article

[View the Full Text HTML](#)

Electrokinetics in Microfluidic Channels Containing a Floating Electrode

Rahul Dhopeswarkar,[†] Dzmitry Hlushkou,[‡] Mark Nguyen,[†] Ulrich Tallarek,^{*,§} and Richard M. Crooks^{*,†}

Department of Chemistry and Biochemistry, Center for Electrochemistry, Texas Materials Institute, Center for Nano and Molecular Science and Technology, The University of Texas at Austin, 1 University Station, A5300, Austin, Texas 78712-0165, Institut für Verfahrenstechnik, Otto-von-Guericke-Universität Magdeburg, Universitätsplatz 2, 39106 Magdeburg, Germany, and Department of Chemistry, Philipps-Universität Marburg, Hans-Meerwein-Strasse, 35032 Marburg, Germany

Received May 15, 2008; E-mail: crooks@cm.utexas.edu; tallarek@staff.uni-marburg.de

Ⓜ This paper contains enhanced objects available on the Internet at <http://pubs.acs.org/jacs>.

We report experiments and simulations on the electrokinetics in a straight microchannel with locally competitive contributions from ionic and electronic conductance due to the presence of an embedded bipolar electrode. The important finding is that this experimentally simple approach can be used to control electric field gradients in microchannels and thus carry out fast analyte enrichment.

Under the conditions reported here, a floating metal electrode in a buffer-filled microfluidic channel nearly eliminates the electric field in its vicinity because of the local dominance of electronic conductance over ionic conductance. However, in adjoining channel segments ionic conductance dominates and extended field gradients develop. The formation of these field gradients is a consequence of the redistribution of ions in the electrolyte solution resulting from electromigration and electroosmotic flow (EOF). We demonstrate these dynamics by observing the migration and concentration enrichment of the twice negatively charged fluorescent dye BODIPY disulfonate. Experimental observations are supplemented with simulations that provide nearly quantitative confirmation of the proposed model.

Details related to the configuration of the microfluidic device and the experimental procedures are provided in the Supporting Information. Briefly, the channel was filled with 5 μM BODIPY disulfonate in 1 mM Tris buffer (pH 8.1). Next, a potential bias was applied between Pt electrodes immersed in ResA (grounded-cathode) and ResB (at a positive potential-anode) to generate an electric field within the channel (Figure 1a). Electrokinetic transport of the dye was captured using an inverted microscope. Figure 1b is an optical micrograph of the Au electrode and microfluidic channel, and Figure 1c is a fluorescence micrograph obtained prior to the application of a potential bias.

Figure 1d shows that when a 50 V bias (~ 5.88 kV/m) is applied the BODIPY dye concentrates to the right of the bipolar electrode. Video 1 shows that dye motion is dominated by EOF and that it opposes electrophoresis. Similar behavior (Supporting Information) was observed for twice negatively charged fluorescein. In contrast, both dyes move uniformly from anode to cathode in the absence of the bipolar electrode due to bulk EOF.¹ This suggests that the EOF in the system with the bipolar electrode, which initially (locally) dominates electrokinetic transport of the dyes, is offset by an increasing magnitude of counter-directional electrophoretic motion as the experiment proceeds. Figure 1e shows the evolution

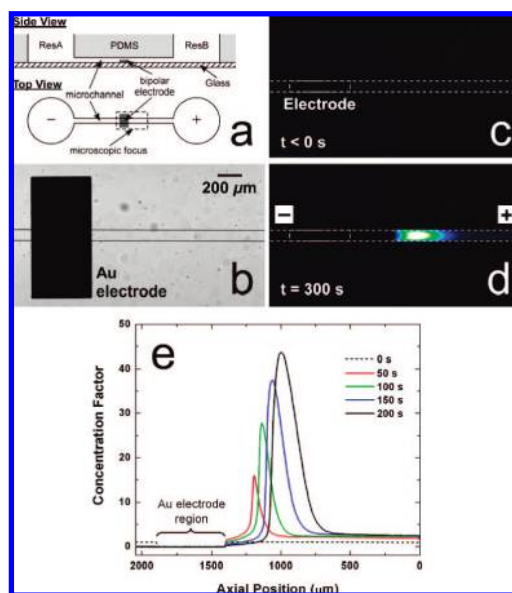


Figure 1. (a) Microfluidic device used in the experiments. The Au electrode ($500 \mu\text{m} \times 1000 \mu\text{m}$) was positioned at the center of the channel (6 mm long, $100 \mu\text{m}$ wide, and $\sim 20 \mu\text{m}$ high) connecting two cylindrical reservoirs (~ 2.5 mm in diameter). (b) Optical micrograph of the Au electrode in the microchannel. Fluorescence micrographs showing variation in the concentration of BODIPY disulfonate in 1 mM Tris-HCl buffer (c) before and (d) after applying a potential of 50 V for 300 s. (e) Concentration profiles for the tracer obtained along the channel during the above experiment (see microscopic focus in Figure 1a). The Au electrode is located from $x = 1400$ to $x = 1900 \mu\text{m}$.

Ⓜ A movie, video 1, shows that dye motion is dominated by EOF and that it opposes electrophoresis.

of the concentrated BODIPY dye zone, which becomes more intense and broader as a function of time.

The complex behavior of bipolar electrodes embedded in microfluidic systems is not well understood, but it has been investigated in some detail recently with an emphasis on faradaic electrochemistry² and induced-charge electroosmosis.³ Yeung and co-workers previously observed analyte enrichment when a Pt wire was inserted into a fused-silica capillary and a bias voltage was applied across that capillary.⁴ They attributed enrichment to a sample sweeping mechanism, which was initiated by electrolysis of water at the ends of the Pt wire. They suggested that this resulted in the formation of a dynamic pH gradient along the capillary, and that this gradient led to spatially resolved acid/base chemistry of the tracer molecules (fluorescein derivatives). A requirement of this

[†] The University of Texas at Austin.

[‡] Otto-von-Guericke-Universität Magdeburg.

[§] Philipps-Universität Marburg.

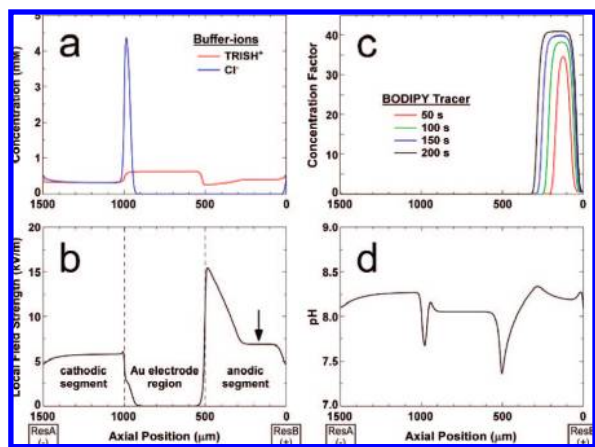


Figure 2. Simulated profiles of (a) background ion concentrations after $t = 200$ s, (b) local axial electric field ($t = 200$ s), (c) tracer concentration for $t = 50$ s, 100 s, 150 s and 200 s, and (d) pH after $t = 200$ s. Applied field strength, $E_{\text{ext}} = 5$ kV/m. All profiles represent the distribution of the corresponding parameter along the geometrical axis of the microchannel. In contrast to Figure 1, the bipolar electrode is located in the microchannel from $x = 500$ to $x = 1000$ μm .

mechanism is that the tracer molecule must be a weak acid and have a pK close to the pH of the buffer. However, the results shown in Figure 1 can not be attributed to this explanation, because BODIPY disulfonate is strongly acidic (two sulfonic acid groups)⁵ and would thus not be sensitive to pH changes in the range required for sweeping methods.

To quantitatively interpret the results presented in Figure 1, we performed numerical simulations based on the coupled Nernst–Planck, Poisson, and the continuity equations, taking into account faradaic reactions and reactions of the buffer system. Figure 1a is a representation of the model used for the simulations. For the simulations, the channel was 1.5 mm long and the electrode was 500 μm long and situated at the center of the channel. To correspond as closely as possible with the experiments, the channel and reservoirs in the simulations were filled with 5 μM BODIPY disulfonate in 1 mM Tris buffer (pH 8.1). The chemical species of interest in this system are neutral Tris, its protonated form (TrisH^+), chloride (Cl^-), hydroxide and hydronium (OH^- and H_3O^+) ions, and the twice negatively charged tracer. Details of the model with partial differential equations, boundary and initial conditions, diffusion coefficients, kinetics of the assumed faradaic and buffer reactions, as well as the system parameters can be found in the Supporting Information. Numerical solutions were obtained for the simulated microfluidic system by employing a parallel code based on lattice algorithms. The results are presented in Figure 2.

Figure 2a and 2b illustrate the close correlation between the concentrations of the background electrolyte ions (TrisH^+ and Cl^-) and the local electric field strength. Specifically, concentration differences of the ions in the anodic channel segment ($x = 0$ –500 μm , Figure 2a) and in the region above the bipolar electrode ($x = 500$ –1000 μm) can be understood in terms of the nonuniformity of the local electric field and hence differences in local transport rates. Because the fluid is assumed to be incompressible, the EOF contribution to ionic flux is constant along the length of the microchannel; however, electromigration is proportional to the local field strength. For cations, these two flux components are codirectional (from ResB to ResA), and hence their sum is proportional to the local field strength. Because field strengths in the anodic and cathodic channel segments and in the region above the bipolar electrode are related by $E_{\text{anode}} > E_{\text{cathode}} > E_{\text{bipolar}}$, the steady-state concentrations of cations in these regions must correspond to C_{bipolar}

$> C_{\text{cathode}} > C_{\text{anode}}$ to conserve charge flux. For anions, the fluxes due to EOF and electromigration are counter-directional and their sum decreases as the local field strength increases and even becomes negative in the anodic segment (i.e., net transport is directed from ResA to ResB). Specifically, Cl^- in the region above the bipolar electrode (low local field strength) is removed toward ResA by the EOF, while Cl^- migrates toward ResB in the anodic segment (high local field strength). This results in a depletion of anions in these two segments ($x = 0$ –1000 μm , Figure 2a). The lower conductivity of the electrolyte solution in the anodic segment leads to the formation of an electric field gradient with field strength increasing from the anode to the right edge of the bipolar electrode (Figure 2b).

The implication of these results is that the tracer molecules, which leave the anodic reservoir because of the initially (locally) dominant EOF, encounter an increasing electrophoretic driving force in the opposite direction (back toward ResB) as they approach the bipolar electrode. At a certain axial position, the two counter-directional motions (anodic electrophoresis vs cathodic EOF) for the tracer are balanced, the molecules become stationary and locally enriched (Figure 2c). The step-like character of the field-strength profile in the anodic segment (arrow in Figure 2b) can be explained by this concentration enrichment of the negatively charged tracer shown in Figure 2c. The tracer concentration becomes comparable with the background ion concentration. As a consequence, the local field strength is a function of the tracer concentration as well as that of the buffer. Following its increase with time, the interplay of fluxes (EOF, electrophoresis, and diffusion) results in a broadening of the concentrated zone.

As pointed out by Yeung and co-workers,⁴ faradaic reactions (e.g., water electrolysis) on the surface of the bipolar electrode induce changes in local pH (Figure 2d), and this can in turn modulate the net charge of analytes having a pK near that of the buffer. In this case, the electrokinetics in the system become more complex and analyte enrichment can be a combined result of the field-gradient mechanism (Figure 2) and a pH-sweeping mechanism.⁴ However, the simulation results, which assume an analyte with pH-insensitive charge, imply that the field-gradient mechanism fully dominates influences of pH change in our experiments (Figure 2d).

In conclusion, a simple bipolar electrode configuration can be used to strongly influence the electric field distribution within a microchannel due to locally competitive contributions of ionic and electronic conductances. Together with the volumetric EOF, these dynamics can be used to generate extended field gradients for tailoring analyte focusing in a simple, straight microchannel. Future experiments will explore the feasibility of extending this observation to combined separations and enrichment.

Acknowledgment. We acknowledge the U.S. Department of Energy, Office of Basic Energy Sciences (Contract No. DE-FG02-01ER15247) for support of this work.

Supporting Information Available: Details of the experimental procedures, micrographs describing concentration enrichment of fluorescein, and a description of the model and the simulations. This material is available free of charge via the Internet at <http://pubs.acs.org>.

References

- (1) Kim, S. M.; Burns, M. A.; Hasselbrink, E. F. *Anal. Chem.* **2006**, *78*, 4779–4785.
- (2) Duval, J. F. L.; Minor, M.; Cecilia, J.; van Leeuwen, H. P. *J. Phys. Chem. B* **2003**, *107*, 4143–4155.
- (3) Squires, T. M.; Bazant, M. Z. *J. Fluid Mech.* **2004**, *509*, 217–252.
- (4) Wei, W.; Xue, G.; Yeung, E. S. *Anal. Chem.* **2002**, *74*, 934–940.
- (5) Videnova-Adrabsinska, V. *Coord. Chem. Rev.* **2007**, *251*, 1987–2016.

JA8036405